13TH NORTH AMERICAN
MASONRY CONFERENCE
JUNE 16-19, 2019 • SALT LAKE CITY, UT, USA

Shake-Table Testing of a Small-Scale Five-Story Confined Masonry Building

Sergio M. Alcocer[1] and Nina Casas[2]

ABSTRACT

The dynamic behavior of a small-scale confined masonry five-story building tested in a shaking table is discussed. The specimen represents a typical low-cost housing building constructed in Mexico. The model was subjected to a series or seismic motions characteristic of Mexican subduction events recorded in the epicentral region. The experimental program, test set-up and instrumentation, and test results are described herein. From recorded and observed results, resisting mechanisms were identified; the structural capacity was assessed in terms of strength, stiffness, deformation and energy dissipation. Response was evaluated and compared to expected performance under the recently published Mexico City Building Code standards for masonry construction and for seismic design.

KEYWORDS: testing, confined masonry, seismic performance, low-cost housing, masonry code

[1] *Professor; Universidad Nacional Autónoma de México; Mexico City, Mexico; salcocerm@ii.unam.mx*
[2] *Graduate Research Assistant; Universidad Nacional Autónoma de México; Mexico City, Mexico; nina_casas@hotmail.com*

Alcocer S. and Casas N. (2019, June). "Shake-Table Testing of a Small-Scale Five-Story Confined Masonry Building." In P.B. Dillon & F.S. Fonseca (Eds.), *Proceedings of the Thirteenth North American Masonry Conference*. Paper presented at the 13th North American Masonry Conference, Salt Lake City, Utah (pp. 121–131). Longmont, CO: The Masonry Society. ISSN 1053-2366.

INTRODUCTION

Confined masonry (CM) is the most common material used for dwelling construction in Mexico and in many Latin American countries. CM consists of load-bearing walls surrounded by small cast-in-place reinforced concrete columns and beams, hereafter referred to as tie-columns (TC) and bond-beams (BB), respectively. TC and BB aim at connecting walls and floor systems to achieve structural integrity.

The seismic behavior of low-rise CM buildings has been generally satisfactory, particularly in epicentral regions where seismic demands are the highest. Nevertheless, significant damages have been observed in near-epicentral regions during strong ground shaking when code-required design and details have not been followed. A typical error is lack of adequate wall confinement due to large spacing between tie-columns, absence of tie-columns at opening edges and insufficient longitudinal and transverse reinforcement in tie-columns and bond-beams. In response to this, performance objectives applicable to confined masonry structures should be assessed, specifically for low-cost and low-rise housing developments (1-6 stories), since these designs are commonly repeated several times and their impact on construction cost is very high.

A series of shaking table tests were previously carried out at UNAM Institute of Engineering shaking table facility. One-story, two-story, and three-story confined masonry specimens were built to half scale following the 2004 Mexican code regulations that have similar strength and detailing requirements to those in the 2017 version (MCBC, 2017). The construction of the five-story specimen is intended to complete the experimental program. The geometry of the five-story specimen is similar to that of the structures previously tested, except for the scale that is 2.4. Layout and detailing are comparable to typical prototypes. A similitude model for ultimate strength was selected as the basis for scaling. To assess the global and local behavior, specimen was instrumented with acceleration, displacement and strain transducers. Non-destructive evaluation methods were applied. A series of earthquake ground motions, characteristic of Mexican subduction events recorded in the epicentral region, were applied through the shaking table. Results are aimed at clarifying our understanding of confined masonry structures seismic behavior and at better estimating the lateral shear resistance of walls subjected to bending demands. Likewise, this test is intended to improve numerical and performance-based models.

EXPERIMENTAL PROGRAM

Description of the specimen

The shaking table system at UNAM is capable of controlling five degrees of freedom and operates in frequencies ranging from 0.1 to 50 Hz. Due to the physical characteristics of the table (4.0 x 4.0 m, and maximum weight of specimens of 196 kN), the model was constructed such that materials for both the model and prototype were identical, thus following the concept of simple dynamic similarity. The model was properly constructed following current Mexican code requirements, since improper detailing is not part of this study. Structure dimensions and are shown in Figure 1. Mechanical and physical properties of the prototype and model materials are given in Table 1. Three wall systems were built in the direction of the earthquake simulator motion (E-W). Facade walls had door and window openings, whereas the middle wall was solid. In the transverse direction (N-S), three walls were built to uniformly distribute gravity loads among walls, to control possible torsional deformations and to improve out-of-plane specimen stability. Model was symmetrical, and the wall distribution was uniform over the specimen height.

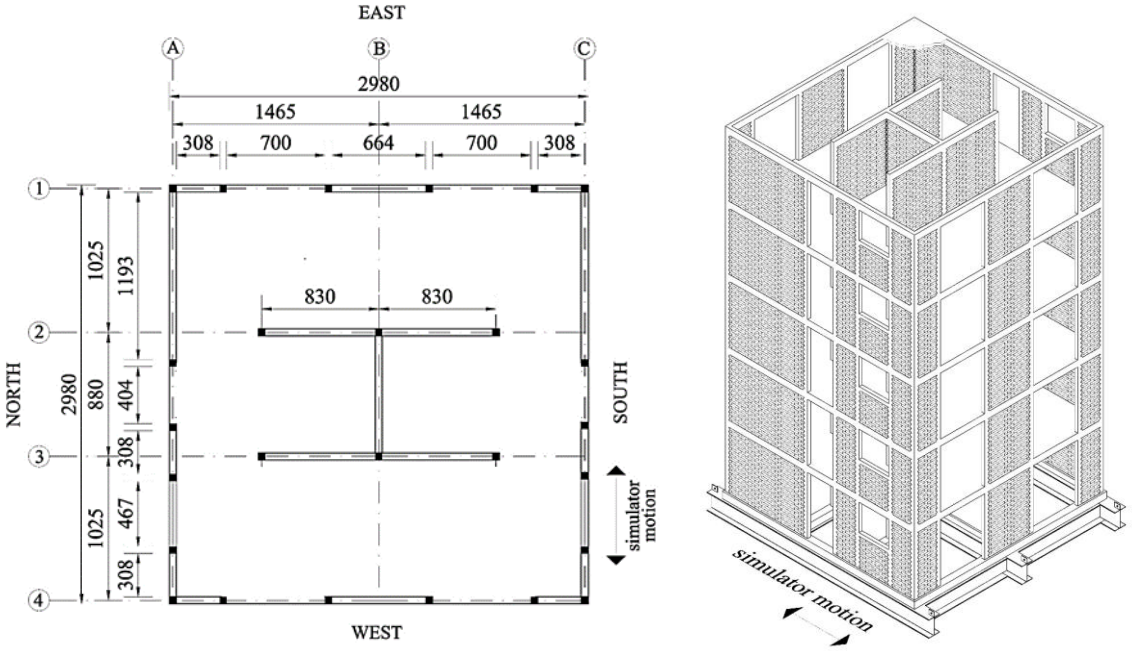

Figure 1. Model plan and 3D view (units in mm)

Materials and construction

The model was built on a steel platform that was bolted to the table. Walls were built with hand-made solid clay bricks confined by reinforced concrete TC and BB. Model clay bricks (50 x 25 x 100 mm) were especially manufactured in a brick factory in Puebla, Mexico. The mortar used to join the units had a cement:lime:sand ratio of 1:0.5:4.5 (by volume) and a specified cube-compression strength of 19.6 MPa. The grading of the sand was scaled down to obtain a maximum size of 1.98 mm. The mortar joint thickness was 4 mm, with a 1-mm tolerance.

Table 1. Physical and Mechanical Characteristics of Prototype and Model

Property, nominal	Prototype	Model
Area in plan, m^2	51.28	8.88
Size of door openings, mm	970 x 2170	404 x 904
Size of window openings, mm	1120 x 1000	467 x 420
Story height, mm	2400	1000
Clay brick size, mm	60 x 120 x 240	25 x 50 x 100
Mortar joint thickness, mm	10	4
TC cross-sectional dimension, mm	120 x 120	50 x 50
BB cross-sectional dimension, mm	230 x 120	96 x 50
Slab thickness, mm	120	50
Size of foundation beams, mm	240 x 240	200 x 100
Diameter of longitudinal steel bars, in. (mm)	3/8 (9.50)	5/32 (3.97)
Diameter of steel bars in hoops, in. (mm)	1/4 (6.35)	5/48 (2.65)
Maximum size of aggregate, in. (mm)	3/4 (19)	5/16 (7.94)
Maximum size of sand grain, mm	4.76	1.98
Nominal strength of concrete, MPa	19.6	19.6
Nominal strength of mortar, MPa	12.3	12.3
Nominal yield stress longitudinal steel, MPa	412	412
Nominal yield stress of hoops, MPa	245	245

Reinforcement layout is shown in Figure 2. TC's and BB's reinforcement was made of four longitudinal deformed wires and of closed hoops spaced at 83 mm; hoop spacing was reduced to 25 mm at TC's ends to increase TC's concrete confinement and shear strength, control damage and, therefore, to achieve a more stable lateral behavior. Floor systems were made of prefabricated solid concrete slabs (floors 1 to 4) and of a cast-in-place reinforced concrete solid slab in floor 5, all cast-integrally to BB. Slabs were reinforced with 3.97-mm diameter deformed wires, spaced each 125 mm in both directions.

Two different types of reinforcing steel wires were used: 3.97-mm (5/32-in.) diameter for TC and BB longitudinal reinforcement and 2.65-mm (5/48-in.) diameter for TC and BB hoop reinforcement. In order to adapt the stress-strain characteristics of original wires to those required by the rules of similarity, a heat-treatment process was required. Steel wires were thermally treated for three hours at a temperature of 1200°F. Bars were tension-tested and a decrease in yield stress was observed (from 677 MPa to 412 MPa). The stress-strain curve of the heat-treated wires was similar to that of low carbon mild steel reinforcement.

For TC and BB, concrete with a cement:gravel:sand ratio of 1:2:1.6 (by weight) was used. Maximum coarse aggregate size was 8 mm and a superplasticizer was used to improve concrete workability and facilitate concrete placement. In order to measure the mechanical properties of the materials, small-scale mortar cubes, concrete cylinders, masonry prisms, and square masonry walls, as well as wire coupons, were sampled. Average measured mechanical properties of materials at 28 days and at the time of testing are shown in Table 2.

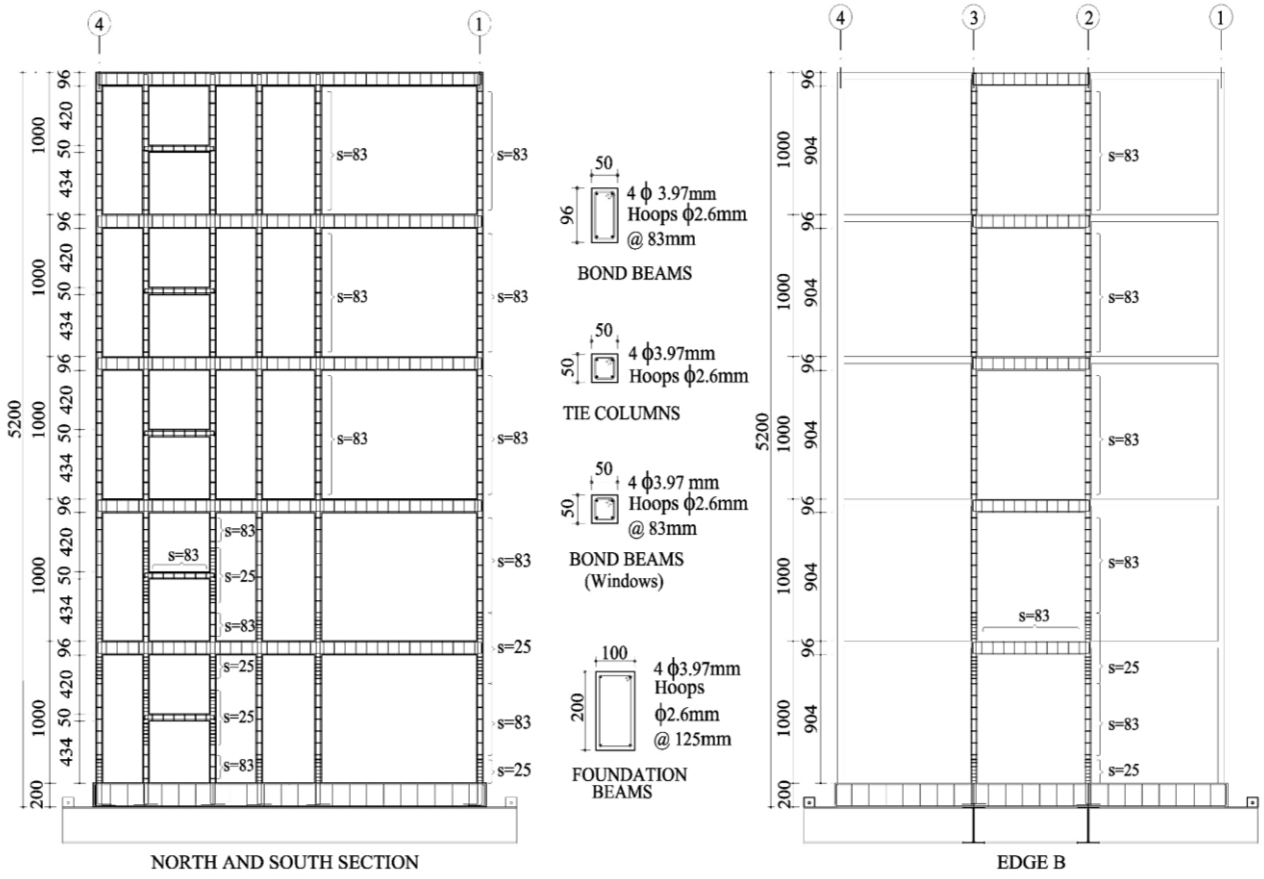

Figure 2. Reinforcement layout

Table 2. Mechanical Properties of Materials (MPa)

Property	28 days	Time of testing
Compressive strength of clay brick units	5.2	5.2
Compressive strength of mortar (cubes)	11.5	15.7
Compressive strength of masonry (prisms)	3.7	3.4
Elastic modulus of masonry (prisms)	1140	1273
Diagonal compression strength of masonry (walls)	0.50	0.50
Shear modulus of masonry (walls)	493.8	375.2
Compressive strength of concrete (cylinders)	24.6	28.4
Elastic modulus of concrete	13,624	19,580
Yield strength of longitudinal reinforcement	355	355
Strength (ultimate stress) of longitudinal reinforcement	530	530
Yield strength of hoop reinforcement	248.5	248.5
Strength (ultimate stress) of hoop reinforcement	396	396

To appropriately model the distribution of masses and live loads in the specimens, 0.50-kN lead ingots were attached to floor slabs. Lead ingots were oriented so that their impact on the slab flexural stiffness and strength was minimized (Figure 3). To correctly simulate the vertical stresses on the walls of the prototype, additional prestressing forces were vertically applied onto the walls of the model and were kept constant throughout the testing program. Prestressing forces were applied through small-diameter (3.2 mm) steel strands. Added mass from strands was deemed insignificant.

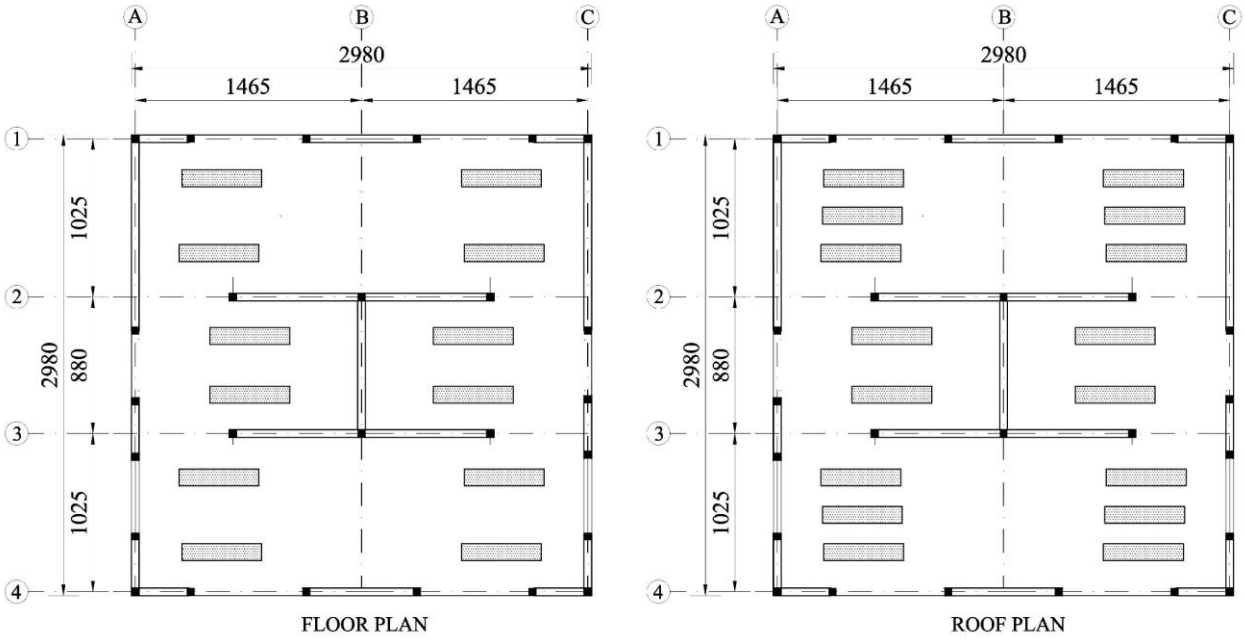

Figure 3. Lead ingots layout in floor plan and roof plan (units in mm)

Instrumentation and test program

To assess the global and local behavior, specimen was instrumented with acceleration, displacement and strain transducers. Story displacements, shaking table and story accelerations, wall deformations and reinforcement strains were recorded during the tests.

Four earthquake motions recorded in epicentral regions in Mexico were used as basis for the testing program. One was that recorded in Acapulco, Guerrero in 1989, during a M=6.8 earthquake (DIANA record). This record was considered as a Green function to simulate larger magnitude events (i.e. with larger instrumental intensity and duration); a M7.6 earthquake was simulated. The second motion was recorded in Fresnillo de Trujano (FTIG record), Oaxaca in 2017 (M=7.2). The other two motions were recorded at San Juan de los Llanos (SJLL record) in Igualapa, Guerrero in 2012 (M=7.2), and at San Luis de la Loma (SLU record), Guerrero in 2014 (M=7.3). Recorded acceleration and duration were scaled to fulfill the requirements of similarity models.

The five-story small-scaled model was subjected to a sequence of seismic excitations by gradually increasing the intensity of motion at each test run up, until the final damage state was attained. A total of 15 test runs were applied and between each test run, a random acceleration signal (white noise) at 50 cm/s^2 (0.05 g) RMS was applied to identify changes in dynamic properties.

TEST RESULTS

Crack patterns

Final patterns of cracking are shown in Figure 4. During SLU record, minor cracking at the base of the wall occurred within the elastic range. At larger intensity motions (SJLL and DIANA records), damage was governed by wall inclined cracking in N and S facades. Simultaneously, horizontal cracks uniformly distributed over the TC and walls on the E and W sides were observed. Damage was characterized, at the end of the tests, by crushing of the masonry walls, cracking and crushing of TC and by wall inclined crack penetration to TC's ends and kinking of TC's longitudinal reinforcement (thus indicating the development of rebar dowel action). Deep cracks and out-of-plane sliding in square walls of N-S facades were observed.

Hysteresis curves

Hysteresis curves in terms of the base shear and lateral drift ratio of the first story are shown in Figure 5, to assess the overall performance of the structure. The base shear was calculated from the measured accelerations at each floor slab center of gravity and by considering the specimen mass and extra mass from lead ingots. Also drawn in the response envelope curve, is the strength prediction using the Mexico City Building Code requirements (MCBC, 2017). The calculation involved measured material properties at time of testing and as-built wall dimensions. The five-story specimen's overstrength level was of the order of 1.60, while the overstrength calculated for the one-story and three-story specimens were 2.0 and 1.3, respectively.

To facilitate comparison among other specimens tested under dynamic or static conditions, three limit states were defined: elastic (E), maximum or strength (M) and ultimate (U). The elastic limit was defined by the occurrence of the first inclined cracking in the masonry wall; strength was achieved when the maximum base shear was resisted; and the ultimate limit state was considered at a lateral drift ratio when 20 percent reduction in strength was recorded.

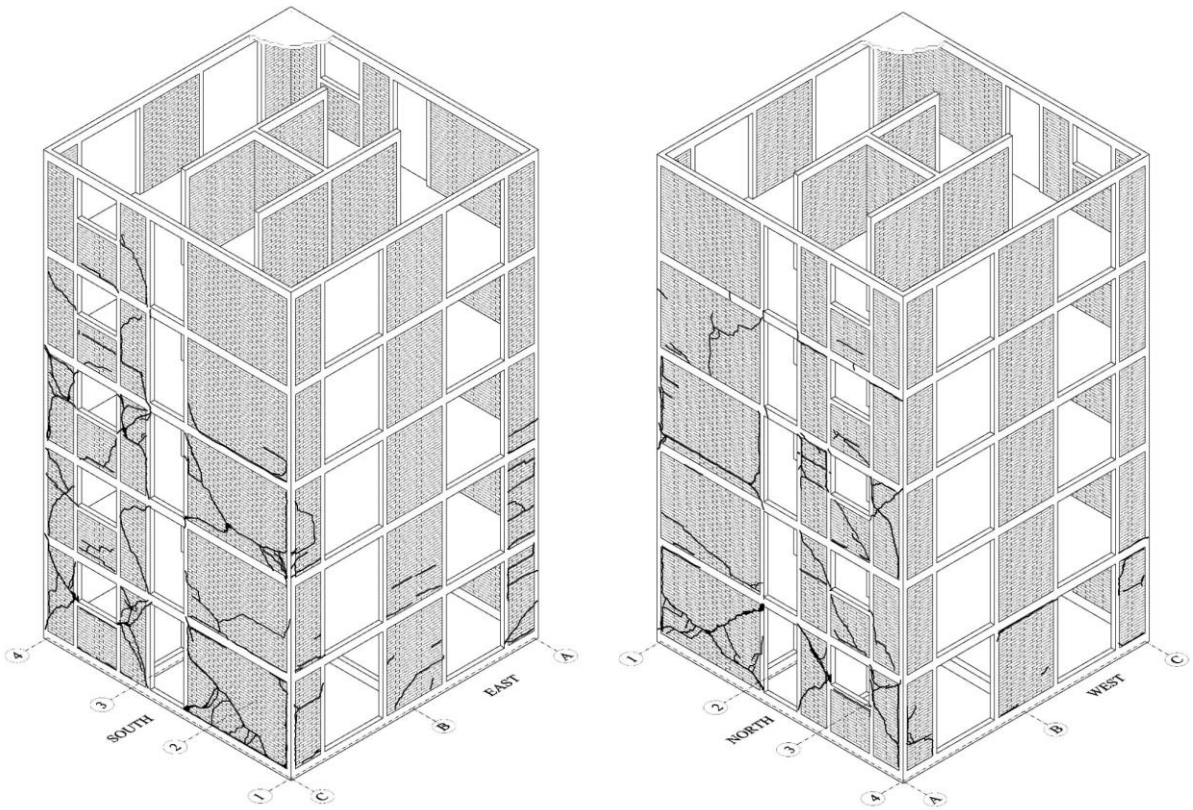

Figure 4. Final crack patterns

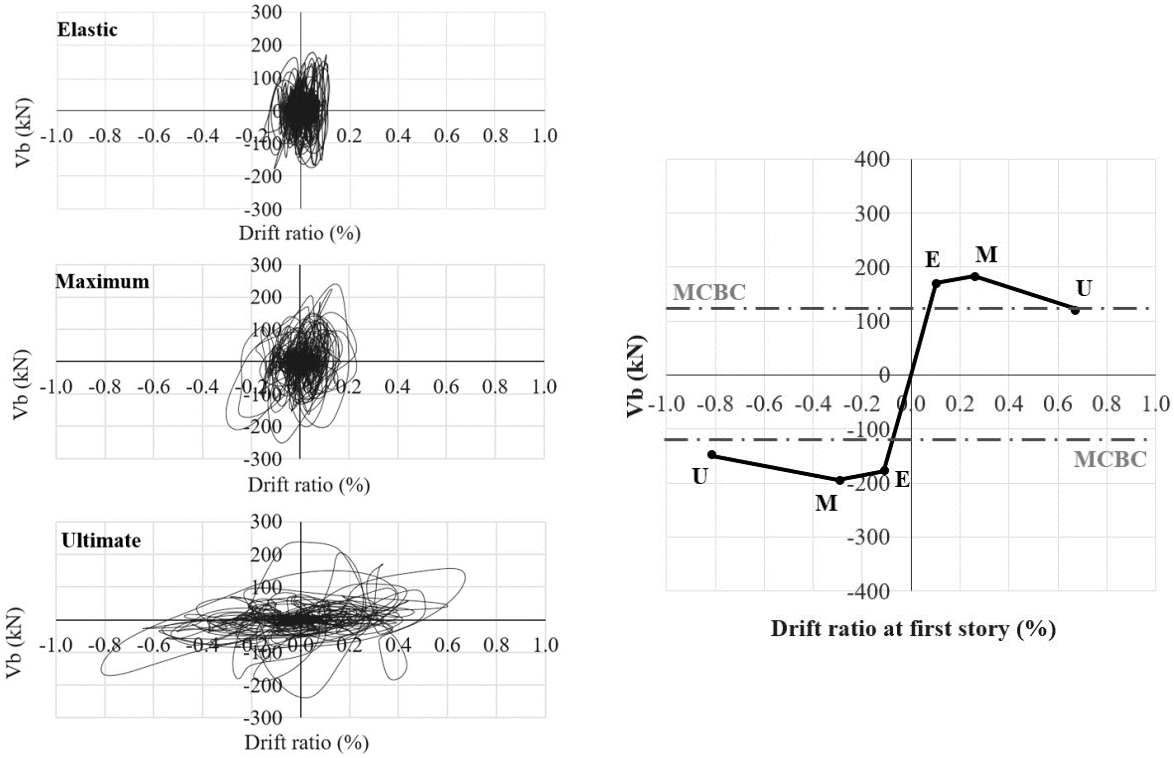

Figure 5. Hysteretic curves and response envelope

Inertial forces at each floor slab were calculated by multiplying the maximum acceleration recorded in the slab center of gravity and the tributary mass of that story. Tributary mass comprised the masses of the slab and lead ingots, plus half the mass of walls above and/or below each story (Figure 6). The shape of the lateral force distribution curves suggested the participation of the first and second modes of vibration. At maximum and ultimate, as expected, larger forces were recorded at the first story.

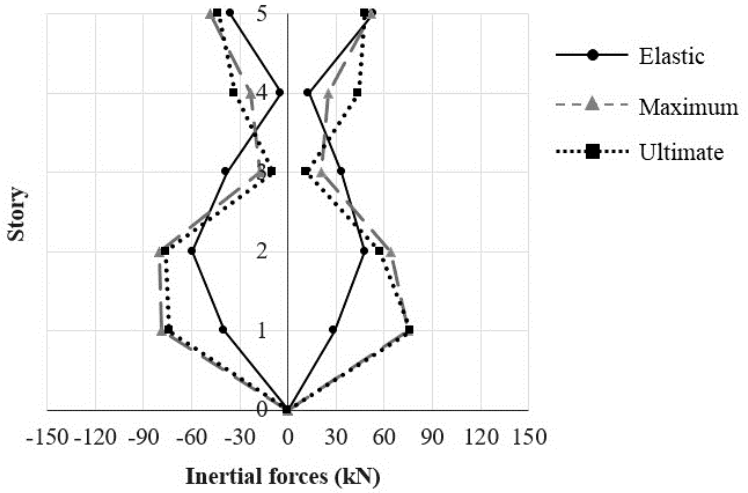

Figure 6. Lateral force distribution for different limit states

Stiffness degradation

Previous test programs have indicated that loss of stiffness is typical even at drift ratios significantly smaller than those at initial inclined masonry cracking. To assess the stiffness degradation phenomenon, peak-to-peak stiffnesses (K_p) were calculated for representative cycles in the model. Results are shown in Figure 7.

Stiffness decay was observed at low drift ratios. This phenomenon is attributed to incipient wall flexural cracking, and perhaps, micro-cracking in masonry materials. After first inclined cracking, the decay increased with drift ratio. At larger drift ratios, K_p remained nearly constant; at this stage stiffness decay is associated to cracking and crushing in masonry walls and reinforced concrete confinement members.

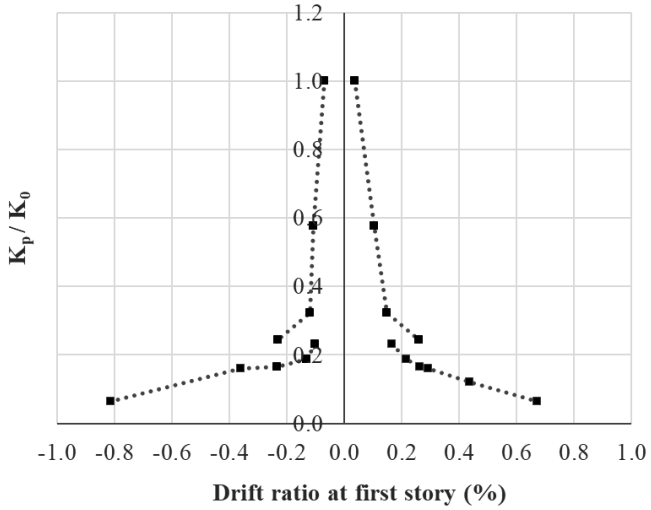

Figure 7. Stiffness degradation

Energy dissipation

The energy dissipated during the tests was computed as the area within the hysteresis loops from base-shear-drift relations. The total cumulative energy dissipated is shown in Figure 8. Test data show three trends on the curve that correspond to the three limit states (elastic, maximum, ultimate). Before the first inclined cracking occurred, very little energy was dissipated since most of this energy was absorbed by the system through elastic deformations.

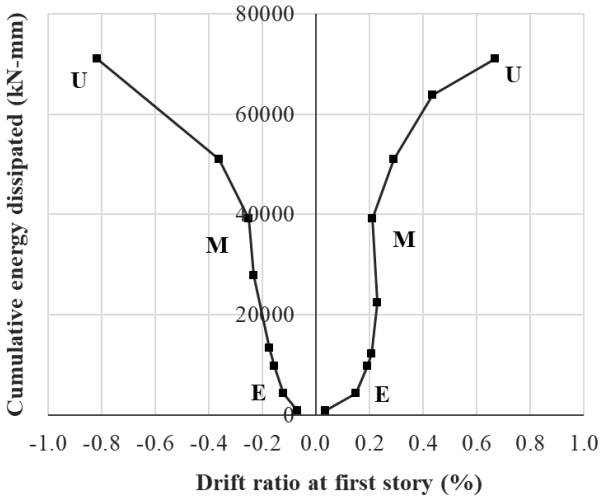

Figure 8. Energy dissipated

Deformation capacity

The deformation capacity of the model was calculated as the ratio between the ultimate displacement and the yield displacement, expressed in terms of drift ratio at first story. For this purpose, Park's equivalent ductility criterion was used (Paulay and Priestley 1992). According to this method, the equivalent ductility is determined from the base shear - drift response envelope, considering as ultimate drift the one corresponding to a strength degradation of 20%. The yield drift is obtained from an initial secant stiffness corresponding to 75% of the yield shear, as shown in Figure 9.

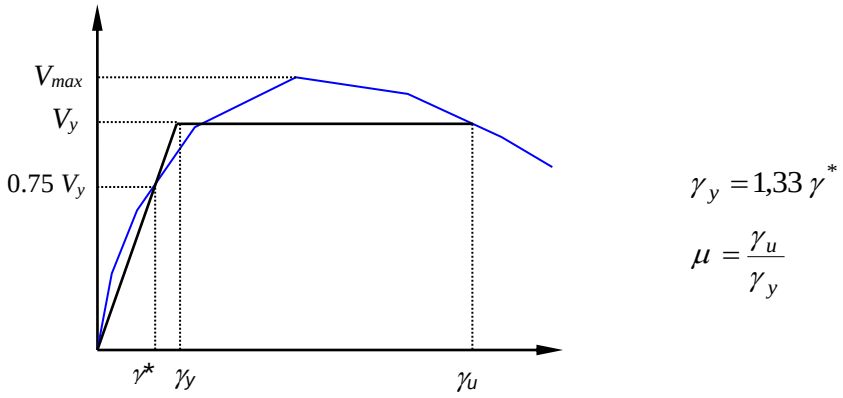

Figure 9. Equivalent ductility according to Park's criterion

The seismic response factor (Q) for CM structures constructed with solid units is specified as Q=2 in the MCBC (2017). Although the seismic coefficient depends not only on the ductility, but also on the hysteretic

energy, an approximate way to obtain this parameter from the calculated ductility is through Equation 1, which is appropriate for short period structures (Newmark and Hall 1982).

$$Q = \sqrt{2\mu - 1} \tag{1}$$

Calculated ductility ratios are shown in Table 3, for envelopes of positive and negative cycles of the first story. Difference in calculated ductility ratios is attributed to the asymmetric response envelopes for positive and negative cycles, caused by the effect of permanent deformations.

Table 3. Equivalent ductility and seismic behavior coefficients

	V_y (kN)	γ_u (%)	γ^* (%)	γ_y (%)	μ	Q
Positive cycles	146.05	0.470	0.067	0.089	5.28	3.09
Negative cycles	156.67	0.700	0.072	0.096	7.29	3.69

CONCLUSIONS

Conclusions are applicable to CM buildings designed and constructed according to present code regulations from Mexico. Based on the failure mode observed, damage was concentrated at the first and third floor, which leads to the assumption that higher modes of vibration can participate in tall CM structures submitted to earthquakes whose frequency content is high. Vibration periods measured before and after the test, showed a decrease in lateral stiffness of the model in the testing direction of about 60%. On the other hand, stiffness degradation of the model obtained from the hysteretic behavior was of the order of 90%. Maximum strength measured during the tests was 60% higher than that calculated with the MCBC (2017). This is consistent with previous observations because design strength is associated to first wall cracking thus neglecting the reserve of resistance that exists between cracking and maximum loads.

Measured stiffness degradation followed an exponential decay, where greater degradation was observed at low seismic intensities (drift values under 0.20%) and decreased progressively for higher intensities. This phenomenon is interesting for seismic design methodologies approaches based on performance, since masonry structures can suffer significant stiffness degradation while submitted to moderate earthquakes. The deformation capacity of the model estimated with Park's criterion, led to a minimum value of drift ductility at the first story of 5.3 and a seismic response factor (Q) of 3.1. This value is comparable with that required in the MCBC (2017) for confined masonry structures, which is adequate if shear deformations concentrated at first story are expected. The drift-cumulative energy dissipated response followed approximately a trilinear curve, coinciding the breaking points with the limit states. Energy dissipated was almost zero before first inclined cracking occurred, however increased at a significant rate afterwards. The highest energy dissipation occurred at final stages where the model exhibited considerable damage.

ACKNOWLEDGMENTS

The financial support of the *Instituto para la Seguridad de las Construcciones en el Distrito Federal*, as well as the donations made by *Grupo CEMEX* and *Cementos Moctezuma*, are acknowledged. The participation of the technical staff of the Shaking Table Laboratory at the Institute of Engineering of the National University of Mexico is thankfully acknowledged.

REFERENCES

Alcocer, S. M. et al. (2004). "Response assessment of Mexican confined masonry structures through shaking table tests," *13th World Conference on Earthquake Engineering*, 2130.

Arias, J. G. et al. (2004). "Respuesta dinámica de modelos a escala 1:2 de viviendas de mampostería confinada de uno y tres pisos, ensayados en mesa vibradora," *XIV Congreso Nacional de Ingeniería Estructural*, II-05, 1-12.

Arias, J. G. (2005). *Ensayos en mesa vibradora de un modelo a escala 1:2 de un edificio de mampostería confinada de tres niveles*, UNAM (master's thesis in Civil Engineering), Mexico City.

Barragán, R. (2005). *Ensaye de una vivienda a escala de dos niveles de mampostería confinada*, UNAM (master's thesis in Civil Engineering), Mexico City.

Barragán, R. et al. (2005). "Comparación de la respuesta dinámica del ensaye de viviendas a escala de uno, dos y tres niveles de mampostería confinada," *XV Congreso Nacional de Ingeniería Sísmica*, VII-01, 1-17.

Mexico Building City Code (MCBC) (2017). *Normas Técnicas Complementarias*, Gaceta Oficial de la Ciudad de México, No. 220 bis, December 15, 2017.

Newmark, N.M. and Hall, W.Y. (1982). *Earthquake Spectra and Design*, Earthquake Engineering Research Institute, Oakland, CA.

Paulay, T. and Priestley, M.J.N. (1992). *Seismic design of reinforced concrete and masonry buildings*, John Wiley & Sons, New York, NY.

Riahi, Z. et al. (2009). "Backbone model for confined masonry walls for performance-based seismic design," *Journal of Structural Engineering*, 135(6), 0733-9445, 644-654.

Vázquez, A. (2005). *Ensaye experimental de viviendas de mampostería confinada de un piso mediante el ensaye en mesa vibradora*, UNAM (master's thesis in Civil Engineering), Mexico City.

Zepeda, J. A. (1999). *Comportamiento ante cargas laterales de muros de ladrillo de arcilla perforado y multiperforado*, UNAM (master's thesis in Civil Engineering), Mexico City.